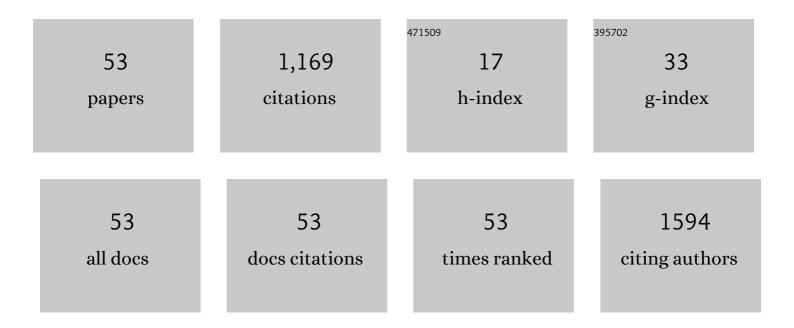
## Merve Meinhardt

List of Publications by Year in descending order

Source: https://exaly.com/author-pdf/968682/publications.pdf Version: 2024-02-01



#	Article	IF	CITATIONS
1	Mueller Matrix-Based Approach for the Ex Vivo Detection of Riboflavin-Treated Transparent Biotissue. Applied Sciences (Switzerland), 2021, 11, 11515.	2.5	4
2	Nonâ€contact remote digital dermoscopy – new perspectives on differential diagnosis of inflammatory skin diseases. Journal of the European Academy of Dermatology and Venereology, 2020, 34, e125-e126.	2.4	4
3	Mueller Matrix Analysis of Collagen and Gelatin Containing Samples Towards More Objective Skin Tissue Diagnostics. Polymers, 2020, 12, 1400.	4.5	5
4	Non-contact fast Mueller matrix measurement system for investigation of bio-tissues. , 2020, , .		0
5	Non-Contact Dermatoscope with Ultra-Bright Light Source and Liquid Lens-Based Autofocus Function. Applied Sciences (Switzerland), 2019, 9, 2177.	2.5	20
6	Optoacoustic inversion via convolution kernel reconstruction in the paraxial approximation and beyond. Photoacoustics, 2019, 13, 1-5.	7.8	2
7	Raman Sensing and Its Multimodal Combination with Optoacoustics and OCT for Applications in the Life Sciences. Sensors, 2019, 19, 2387.	3.8	17
8	Single Transparent Piezoelectric Detector for Optoacoustic Sensing—Design and Signal Processing. Sensors, 2019, 19, 2195.	3.8	13
9	Multivariate discrimination of heat shock proteins using a fiber optic Raman setup for <i>in situ</i> analysis of human perilymph. Review of Scientific Instruments, 2019, 90, 043110.	1.3	2
10	Mueller Matrix Measurement of Electrospun Fiber Scaffolds for Tissue Engineering. Polymers, 2019, 11, 2062.	4.5	15
11	Monte Carlo simulation of the influence of internal optical absorption on the external Raman signal for biological samples. Journal of the Optical Society of America A: Optics and Image Science, and Vision, 2019, 36, 877.	1.5	7
12	Modeling of Raman-Scattering Signals in Biological Tissues by Direct and Two-Step Approaches. Optics and Spectroscopy (English Translation of Optika I Spektroskopiya), 2018, 124, 180-186.	0.6	2
13	Trimodal system for in vivo skin cancer screening with combined optical coherence tomographyâ€Raman and colocalized optoacoustic measurements. Journal of Biophotonics, 2018, 11, e201700288.	2.3	34
14	Numerical prediction and measurement of optoacoustic signals generated in PVA-H tissue phantoms. European Physical Journal D, 2018, 72, 1.	1.3	6
15	In vivo determination of carotenoid resonance excitation profiles of <i>Chlorella vulgaris</i> , <i>Haematococcus pluvialis</i> , and <i>Porphyridium purpureum</i> . Journal of Raman Spectroscopy, 2018, 49, 404-411.	2.5	9
16	Absorption and resonance Raman characteristics of <i>β</i> -carotene in water-ethanol mixtures, emulsion and hydrogel. AIP Advances, 2018, 8, .	1.3	15
17	Polymer Based Whispering Gallery Mode Humidity Sensor. Sensors, 2018, 18, 2383.	3.8	18
18	Violaxanthin cycle kinetics analysed <i>in vivo</i> with resonance Raman spectroscopy. Journal of	2.5	9

Raman Spectroscopy, 2017, 48, 686-691.

Merve Meinhardt

#	Article	IF	CITATIONS
19	Comparative study of presurgical skin infiltration depth measurements of melanocytic lesions with OCT and high frequency ultrasound. Journal of Biophotonics, 2017, 10, 854-861.	2.3	32
20	Development of a combined OCT-Raman probe for the prospective <i>in vivo</i> clinical melanoma skin cancer screening. Review of Scientific Instruments, 2017, 88, 105103.	1.3	33
21	A non-contact remote digital dermoscope to support cancer screening and diagnosis of inflammatory skin disease. Biomedical Physics and Engineering Express, 2017, 3, 055005.	1.2	15
22	Efficient procedure for the measurement of preresonant excitation profiles in UV Raman spectroscopy. Review of Scientific Instruments, 2017, 88, 073105.	1.3	5
23	All-polymer whispering gallery mode sensor for application in optofluidics. Optical Data Processing and Storage, 2017, 3, .	3.3	2
24	Iterative morphological and mollifier-based baseline correction for Raman spectra. Journal of Raman Spectroscopy, 2017, 48, 336-342.	2.5	40
25	Polymer WGM arrays for optical sensing applications. , 2017, , .		0
26	Towards a multimodal device for clinical in-vivo skin cancer depth measurements. , 2017, , .		0
27	Simulation of Raman scattering including detector parameters and sampling volume. Journal of the Optical Society of America A: Optics and Image Science, and Vision, 2017, 34, 2138.	1.5	4
28	Optical properties of the human round window membrane. Journal of Biomedical Optics, 2017, 22, 1.	2.6	1
29	Monte Carlo simulation of Raman confocal spectroscopy of beta-carotene solution. , 2016, , .		0
30	Confocal Raman microscopy and fluorescent in situ hybridization – A complementary approach for biofilm analysis. Chemosphere, 2016, 161, 112-118.	8.2	15
31	Surface-immobilized whispering gallery mode resonator spheres for optical sensing. Sensors and Actuators A: Physical, 2016, 252, 82-88.	4.1	7
32	Simple model to simulate OCT-depth signal in weakly and strongly scattering homogeneous media. Journal of Optics (United Kingdom), 2016, 18, 125302.	2.2	11
33	UV-resonance Raman spectroscopy of amino acids. , 2016, , .		0
34	Two efficient approaches for modeling of Raman scattering in homogeneous turbid media. Journal of the Optical Society of America A: Optics and Image Science, and Vision, 2016, 33, 426.	1,5	12
35	All-polymer whispering gallery mode sensor system. Optics Express, 2016, 24, 6052.	3.4	11
36	LEDs for energy efficient greenhouse lighting. Renewable and Sustainable Energy Reviews, 2015, 49, 139-147.	16.4	327

Merve Meinhardt

#	Article	IF	CITATIONS
37	Light source design for spectral tuning in biomedical imaging. Journal of Medical Imaging, 2015, 2, 044501.	1.5	10
38	Cladded self-written multimode step-index waveguides using a one-polymer approach. Optics Letters, 2015, 40, 1830.	3.3	34
39	Temperature-sensitive gating of hCx26: high-resolution Raman spectroscopy sheds light on conformational changes. Biomedical Optics Express, 2014, 5, 2054.	2.9	21
40	Tissue phantoms for multimodal approaches: Raman spectroscopy and optoacoustics. , 2014, , .		4
41	Sewerage tunnel leakage detection using a fibre optic moisture-detecting sensor system. Sensors and Actuators A: Physical, 2014, 220, 62-68.	4.1	41
42	Lighting with laser diodes. Advanced Optical Technologies, 2013, 2, 313-321.	1.7	68
43	An ultra-bright white LED based non-contact skin cancer imaging system with polarization control. , 2013, , .		2
44	Combining optoacoustics and resonance Raman spectroscopy for quantification of biomolecules in situ. , 2012, , .		0
45	A computational model for previtamin D3 production in skin. Photochemical and Photobiological Sciences, 2012, 11, 731-737.	2.9	11
46	Hierarchical Cluster Analysis (HCA) of Microorganisms: An Assessment of Algorithms for Resonance Raman Spectra. Applied Spectroscopy, 2011, 65, 165-173.	2.2	36
47	Of microparticles and bacteria identification – (resonance) Raman micro-spectroscopy as a tool for biofilm analysis. Water Research, 2011, 45, 4571-4582.	11.3	27
48	Effects of ethanol, formaldehyde, and gentle heat fixation in confocal resonance Raman microscopy of purple nonsulfur bacteria. Microscopy Research and Technique, 2011, 74, 177-183.	2.2	24
49	Absorption Spectra of Human Skin <i>In Vivo</i> in the Ultraviolet Wavelength Range Measured by Optoacoustics. Photochemistry and Photobiology, 2009, 85, 70-77.	2.5	26
50	Effect of ultraviolet adaptation on the ultraviolet absorption spectra of human skin <i>in vivo</i> . Photodermatology Photoimmunology and Photomedicine, 2008, 24, 76-82.	1.5	18
51	Wavelength-dependent penetration depths of ultraviolet radiation in human skin. Journal of Biomedical Optics, 2008, 13, 044030.	2.6	150
52	Optoacoustics, laser-induced fluorescence (LIF), and photometry for investigation of different skin types in vitro and in vivo. , 2003, 5143, 50.		0
53	<title>Investigation of optical properties of human skin in the UV</title> ., 2002, , .		Ο